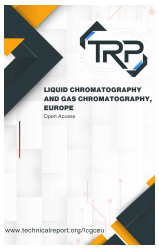

Journal of Liquid Chromatography and Gas Chromatography, Europe
https://technicalreport.org/lcgceu/

LC GC Eu., Vol. 39, No.2, 11-23, 2026

Technical Reports Press

RESEARCH ARTICLE

Sugar State Measurability via NiFe Nanowire Chronoamperometry in Foods

Louis E. Brus[1*] **and Beckstein Biggin**[1]

[1]*Department of Chemistry, Columbia University, New York, New York 10027, USA*
[*]*Corresponding author*

Corresponding author:
leb26@columbia.edu

Received: 11 January 2026
Accepted: 09 May 2026
Available online: 30 June 2026

Abstract
The usefulness of the reported quantity in a food matrix relies on the fact that it should maintain the same chemical condition as that responsible for the current response. Therefore, this work seeks to explore whether the NiFe nanowire chronoamperometry can be able to report three kinds of output from a food sample, which include a single concentration for a specific reducing-sugar class, a range of concentration for an unclassifiable reducing-sugar class, and the total sugar content after conversion. In doing so, the calculations will employ calibration and validation values for glucose, fructose, galactose, lactose, maltose, sucrose after pre-treatment, and food samples of peach juice, honey, milk, isotonic solution, coke, diet coke, and apple. These values will be organized using RLC, CBCE, HGP, and RTA without adding a new laboratory procedure. The first common linear calibration interval of these sugars and foods was between 0.05 mM and 0.30 mM. Glucose, fructose, and galactose belong to the high responding monosaccharides having the mean sensitivity of 0.6427 μA μM^{-1} cm^{-2}, and lactose, and maltose belong to the low responding disaccharides with a mean sensitivity of 0.3555 μA μM^{-1} cm^{-2}. Consequently, the class multiplier becomes 1.81, implying that an unknown class current difference can only be reported as a concentration after specifying its chemical condition. Monosaccharides and disaccharides have mean RLC of 0.9168 and 0.6175 respectively. The mean recovery values in the food validation were 98.05% for reducing sugar and 99.11% for total sugar. Hydrolysis contribution of the peach-juice and apple was 67.36% and 38.44% respectively. Therefore, the response by the NiFe nanowire is fit for food quality determination when the reported value is clearly specified with regard to sugar class and conversion state.

Keywords: NiFe nanowires, reducing sugars, total sugar, non-enzymatic electrochemical sensor, calibration reliability, hydrolysis gain, food analysis

1. Introduction

Measurement of sugar content in foods raises both analytical and reporting challenges. Juice, honey, milk, soda, and isotonic solutions may all contain electroactive carbohydrates, but their meanings in the resulting concentration statements are specific to the class of sugar and food preparation. Glucose, fructose, and galactose are the monosaccharide reducing sugars; lactose and maltose are disaccharide reducing sugars; sucrose does not produce an electrochemical signal in direct alkaline chronoamperometric measurement unless it undergoes conversion to another form. Food-composition science on total, added, and free sugars emphasizes that there is no interchangeability between the label, nutritional, and process-control meanings of sugar statements [1,2]. A one-dimensional amperometric measurement becomes scientifically meaningful only when the authors declare whether it relates to direct reducing sugar, reducing sugar equivalent of particular class, or total sugar after conversion.

Reviews on recent electrochemical sensor development for the food industry highlight the benefits of these techniques [3,4] – small sample sizes, short analysis time, portable readout, low power consumption, and decentralization of quality control. Fast analysis of reducing sugars and electrochemical assays for food are clear illustrations of the practicality of such sensors [5,6]. Applications in process monitoring and miniaturization of devices also demonstrate integration of sugar analysis in dairy analysis and miniature electrochemical devices [7,8]. The advantages become particularly valuable for food production fa-

Cite as: L. E. Brus and B. Biggin. Sugar State Measurability via NiFe Nanowire Chronoamperometry in Foods. LC GC Eu., 39(2) 2026: 11-23.

cilities, as repeat analyses may be required in the process of ingredient reception, adjustment of process parameters, fermentation control, beverages blending, or testing of release products. Conventional chromatography and spectrometry remain important due to their ability to detect separate carbohydrates or serve as standard laboratory validation tests [9, 10], but these procedures require more complex sample preparation and instrumentation. Electrochemical sensing is not the universal alternative to sugar analysis by separation [11], but it is valuable for fast screening as long as the concentration statement does not lose the chemistry of the sample.

The field of glucose sensing without enzymes has grown rapidly using materials such as metal oxides and metal sulfides [12], transition metal systems [13], and alloys, layered hydroxides, carbon-based catalysts, and conductive composites [14, 15]. Foundational investigations established basic performance criteria for glucose sensors without enzymes [16]. Typical characteristics include sensitivity, detection limit, measuring range, response time, stability, and anti-interference behavior. Such features are necessary, but not sufficient in the context of sugar content reporting for foods when the target is not a single known analyte. An excellent glucose electrode can give a wrong report on sugar concentration in a food containing predominantly lactose in dairy products, fructose in fruits, or sucrose in beverages. The point is important since enzyme-free sensors do not utilize biological recognition of a single carbohydrate, but rather depend on interfacial oxidation of electroactive substances on catalytic surfaces.

Nickel-containing electrodes are widely used in non-enzymatic carbohydrate sensing because of redox properties of nickel hydroxide and nickel oxyhydroxide [17]. Studies of mechanistic processes in such systems revealed that nickel–iron interactions change redox properties and catalytic behavior of nickel [18, 19]. Recent material studies demonstrated that such structures as layered hydroxides [20], carbon-supported Ni/NiO composites [21], ordered nickel nanowires and NiCo composites [22, 23], and nickel hydroxide electrodes [24] give excellent enzyme-free glucose response when surface area, conductivity, morphology, and electronic coupling are controlled. The case of NiFe material is particularly important since iron changes the electronic and redox environment of nickel and nanowire morphology provides high area and vertical ordering of electrode surface. Similar to other materials, the same design features increase the importance of proper calibration, since the differences in surface accessibility, diffusion, active sites availability, and molecular sizes for glucose, fructose, galactose, lactose, and maltose exist.

Measurements using NiFe alloy nanowires are especially appropriate for reporting-centred analysis, as they combine electrode structure, sugar calibration, and validation of food samples. The electrode was produced by template-assisted electrodeposition to obtain ordered NiFe nanowires on a nickel current collector. Nanowires have a diameter of 246.5 ± 16.5 nm, length of 11.4 ± 0.55 μm, and Fe/Ni ratio of 79/21 at%. Double layer capacitance is 50 times higher than in case of planar nickel and 20 times higher than in case of NiFe alloy on nickel foil, which proves high surface area of the nanowires. Chronoamperometry was carried out in 0.1 M NaOH with applied potential of +0.5 V versus SCE. Response time is near 6 s [11]. The measured values include five reducing sugars, weak direct response of sucrose before conversion, screening of interferents, stability and reactivation experiments, and validation of foods such as juice, honey, milk, isotonic solution, coke, diet coke, and apple.

Hence, the question of the study is specific and concerns the condition under which the response of NiFe nanowire sensor is reported as a single value, as an interval, or after conversion to total sugar. The question is different from the ranking of material sensitivity since it is focused on the reportable sugar state as an object of analysis. Numerical basis of the study consists of five rows with sugar calibrations, direct reducing-sugar values in food samples, total sugar values in food samples, paired direct/total matrices, recovery quantities, and deployment examples. RLC, CBCE, HGP, and RTA are used as calculations that maintain the reportable concentration compatible with sugar chemistry, conversion status, and agreement of food-matrix pair. The reporting-focused approach is important because single-channel amperometry cannot alone distinguish sugar mixture. Sensor arrays and chemometric techniques can provide mixture separation when several independent measurements are available [25, 26]. One-channel current trace of NiFe nanowire contains different information: it gives fast oxidation response which is interpreted through class knowledge, calibrated bounds, or pre-treatment status. The central achievement of the study is the link between electrode performance and reportable states of food-sugars. This link is essential for quality control, since the concise result should be informative about the actual measured sugar state.

2. Materials and Methods

2.1. Electrode Values and Analytical Organization

The analysis takes advantage of the published NiFe alloy nanowire sugar electroanalysis values used for total sugar determination in food. The values are provided as records including electrode fabrication and characterization data, electrochemical operating parameters, sugar-specific calibration descriptors, food-matrix validation data, sucrose pre-treatment data, interference study data, stability/reactivation data, and comparisons with nickel-based sensors [11]. The analysis does not introduce any new laboratory method; it provides an improved interpretation of the published numeric record, keeping sugar class, conversion state, and matrix agreement evident throughout the paper.

The electrode must be described as an ordered NiFe nanowire array, not an unspecified nickel surface. A thin gold layer was sputtered on a nanoporous polycarbonate membrane to form a conductive template. Nickel was deposited at -1.5 V vs. SCE for 90 min from a Watt-type bath with nickel sulphate, nickel chloride, and boric acid. NiFe nanowires were deposited from the $FeSO_4$-modified Watt bath under a pulsed potential regime between -0.65 V and -1.35 V vs. SCE for 100 cycles. The polycarbonate template was dissolved in chloroform by repeated solvent treatments. The electrode structure matches the electrochemical operation in the 3D-printed electrochemical cell with up to 4 mL of solution volume, a working electrode area of 0.785 cm^2, 1 mm microfluidic channels, peristaltic pump-based mixing, a platinum counter electrode, and a saturated calomel reference electrode. Thus, the electrode should be regarded as an ordered nanowire structure, not as an unspecified NiFe deposit.

The analysis was organized in four layers. The first layer was a sugar-specific calibration layer with glucose, fructose, galactose, lactose, and maltose. For each sugar, the first linear range was 0.05–0.3 mM, and the descriptors were sensitivity, repeatability, reproducibility, limit of detection (LOD), and limit of quantification (LOQ). The second layer was a class layer grouping glucose, fructose, and galactose as monosaccharides and lactose and maltose as disaccharides. The third layer was a food-matrix layer with direct reducing-sugar data and total sugar data after pre-treatment. The fourth layer was a deployment layer with comparison of the NiFe nanowire measurements with representative NiFe-based systems [27, 28], NiCu and NiCo-based architectures [29, 30], cobalt-nickel sulfides [31], ordered nickel nanowires [22], and recent NiCo or nickel hydroxide electrodes [23, 24].

The physical measurement platform is shown in Figure 1 prior to introduction of reliability calculations. The nanowire dimensions, alloy composition, electrochemical cell geometry, and electroactive area contrast provide the material basis for the subsequent sugar response calculation.

The electrode picture should be regarded as the physical justification of treating the response as the measurement on the nanowire array. The high aspect ratio, alloy composition, and cell geometry provide

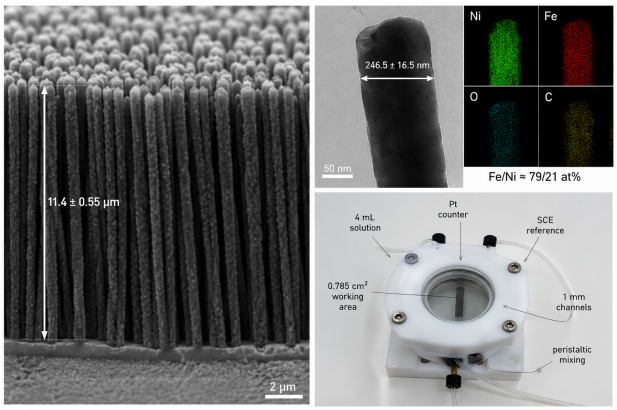

Figure 1: NiFe nanowire electrode and cell.

the explanation for the use of current density, not only mass-based descriptor in the following calibration analysis. The electrode is the high-area NiFe interface used in the specific alkaline cell, not an unspecified nickel surface.

The operating chemistry is summarized in Figure 2. It emphasizes the alkaline electrolyte, +0.5 V vs. SCE working potential, fast current response, and distinct treatment of reducing sugars and sucrose prior to calibration.

The measurement environment clarifies why the further analysis distinguishes between reducing-sugar class and conversion state. The fast current rise in alkaline solution indicates the possible use in screening, but the weak response of sucrose demonstrates that total sugar cannot be estimated based on the direct reducing-sugar measurement only. This distinction represents the chemical reason of keeping the direct and converted responses separate.

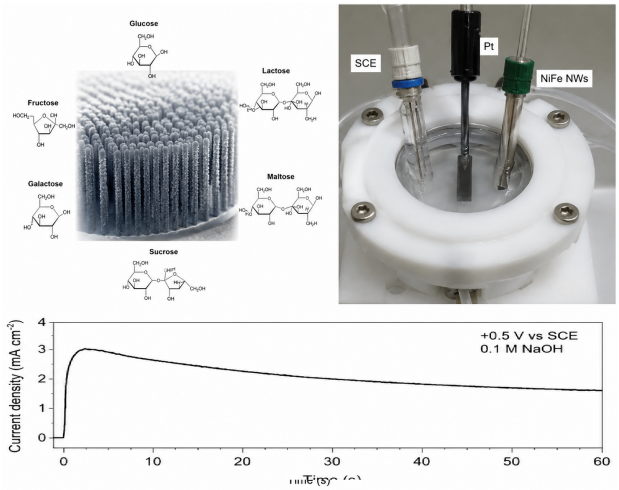

Figure 2: Alkaline sugar-response environment.

2.2. Reliability-Ledger Calibration

Reliability-Ledger Calibration (RLC) was applied to map the reported calibration information into an analyte-specific dimensionless reliability index. Given the analyte i, the current density increment in a chosen linear range is denoted as

$$\Delta J_i = S_i C_i, \tag{1}$$

where ΔJ_i is blank-corrected current density increment, S_i is sensitivity and C_i is analyte concentration. The first shared linear range starts with $C_L = 50\ \mu$M. Thus, detection reserve and quantification reserve are given by the relations

$$D_i = \frac{C_L}{LOD_i}, \qquad Q_i = \frac{C_L}{LOQ_i}. \tag{2}$$

Neither detection reserve nor quantification reserve can substitute LOD and LOQ. They represent the excess of the starting point of the operating range over detection and quantification limits, respectively. The definition corresponds to the accepted analytical practice, according to which the detection capacity is relevant only in the context of particular measurement range [32, 33].

Finally, repeatability and reproducibility measures were employed to form a precision-retention term:

$$P_i = 1 - \frac{r_i + R_i}{200}, \tag{3}$$

where r_i and R_i are percentages. The denominator provides the simple upper-bound penalty: as soon as the repeatability and reproducibility losses are low, the value of P_i is almost one, and the reliability index drops when they increase. Thus, the analyte reliability index is

$$\Lambda_i = \left[\left(\frac{S_i}{\max_j S_j} \right) \left(\frac{\min_j LOD_j}{LOD_i} \right) P_i \right]^{1/3}. \tag{4}$$

Geometric mean was chosen since it does not allow for a highly sensitive method to overshadow the lack of sensitivity reserves or the imprecision of the method. This is not meant to be an universal regulation parameter but rather a comparative value to compare the five sugars within the same calibration set.

2.3. Class-Bound Concentration Enveloping

Class-Bound Concentration Enveloping (CBCE) is utilized for estimating the concentration of unknown-class samples without an additional laboratory test step. $\bar{S}_{mono}$ represents the mean sensitivity of glucose, fructose, and galactose, and $\bar{S}_{di}$ represents the mean sensitivity of lactose and maltose. The current-density increment, ΔJ, is transformed into the class-related concentration using the following equation:

$$\widehat{C}_g = \frac{\Delta J}{\bar{S}_g}, \tag{5}$$

where g represents the molecular class of sugar. In order to convert the current density increment to class-specific concentration, it should be noted that the monosaccharide mean slope is greater than the disaccharide mean slope. Therefore, the same value of ΔJ leads to a smaller estimate of concentration under monosaccharide calibration and a larger estimate under disaccharide calibration. In case of unknown matrix class, the resulting concentration is presented in the form of a class-bound interval,

$$\mathscr{B}(\Delta J) = \left[\frac{\Delta J}{\bar{S}_{\text{mono}}}, \frac{\Delta J}{\bar{S}_{\text{di}}} \right]. \tag{6}$$

The class-expansion multiplier is defined as
The class-expansion multiplier is

$$M_{CBCE} = \frac{\bar{S}_{mono}}{\bar{S}_{di}}, \tag{7}$$

and the percentage expansion of the upper bound over the lower bound is

$$E_{CBCE} = 100(M_{CBCE} - 1). \tag{8}$$

This quantity is independent of the absolute current increment. It gives the reporting penalty associated with unknown molecular class.

2.4. Hydrolysis-Gain Partitioning

The Hydrolysis-Gain Partitioning (HGP) method was applied to matrices which can be analyzed in direct reducing sugar and total sugar modes. If $C_{R,k}$ is the concentration of the direct reducing sugars of matrix k and $C_{T,k}$ is the concentration of total sugars after conversion, the hydrolysis gain is defined as

$$H_k = \frac{C_{T,k}}{C_{R,k}}. \tag{9}$$

The fraction of the total signal corresponding to the conversion is

$$\phi_k = 100\left(\frac{C_{T,k} - C_{R,k}}{C_{T,k}}\right). \tag{10}$$

For matrices having both sensor and reference data, the difference between two estimates of the partitioning is

$$\Delta\phi_k = \phi_{sensor,k} - \phi_{ref,k}. \tag{11}$$

This approach is required because total sugar measurement is more than just replication of the direct measurement of reducing sugars. It requires determination if conversion uncovers a significant latent component and if the sensor-based partition matches the reference partition. This approach is in keeping with the general division into total, added, free, and reducing sugars in food reporting [1, 2].

2.5. Recovery-Tension Analysis

The Recovery-Tension Analysis (RTA) framework was applied to interpret agreement in real samples. Recovery was defined as a percentage agreement between the NiFe sensor value and a reference (or label) value. In this case, the residual is

$$\varepsilon_k = Rec_k - 100, \tag{12}$$

where Rec_k is the published recovery for food-mode entry k. Normalized recovery-tension indicator is

$$T_k = \frac{|\varepsilon_k|}{5}. \tag{13}$$

The denominator defines a common interpretation range of $\pm 5\%$ used for comparison of entries in the same measurement set; the latter is not claimed to be a technical specification. Values less than one indicate that the residual falls into the chosen range, and values greater than one indicate the need for explanation of the entry. Also, for entries where both sensor and reference standard deviations were provided, normalized residual based on uncertainty was calculated:

$$z_k = \frac{C_{sensor,k} - C_{ref,k}}{\sqrt{\sigma^2_{sensor,k} + \sigma^2_{ref,k}}}. \tag{14}$$

This value helps to distinguish a large percentage residual from a difference small compared to the measurement system's uncertainty. Interpretation is based on the methodology-validation approach when recovery and trueness are evaluated with respect to application and uncertainty of the measurement system [34].

2.6. Deployment Comparison

The deployment comparison did not use minimum LOD alone to compare the performance of various sensor designs. It took analyte breadth, matrix breadth, and reporting mode into account. This is important in the case of food analysis where sugar levels in foods are much higher than the micromolar detection limits. Dilutions are necessary in order to calibrate the readings into a proper range. The very low LOD is useful in such circumstances, but it is not the only descriptor in food sugar analysis that is meant to separate direct reducing sugars, total sugars after conversion, and calibrating by classes. Comparative entries were thus viewed as being glucose-based, multi-sugars, biological matrices, food matrices, or total sugars capable works. Nickel nanoflowers and NiO/CNT electrodes represented the early nickels sugar sensing platforms [35, 36]. NiFe layered hydroxides and NiFe-polyanilines represented Fe-nickel structures [27, 28]. NiCu and NiCo structures extended the bimetallic comparisons [29, 30]. Cobalt-nickel sulfides and trehalose oriented nickel foams added to the matrices and analyte variety [37]. Ordered nickel nanowires and non-invasive NiCo structures contributed to the deployment differences [22, 23]. Nickel hydroxide electrodes rounded off the comparisons [24].

3. Results and Discussion

3.1. Calibration Descriptors Establish a Class-Separated Response

Table 1 presents the set of sugar-specific parameters that were included in the calculation of the RLC. It should be noted that all five sugars possess identical first linear concentration range, however, response magnitude of five analytes splits into two groups. Glucose was characterized by maximum sensitivity (0.710 μA μM^{-1} cm^{-2}), whereas fructose (0.610) and galactose (0.608 μA μM^{-1} cm^{-2}) were less sensitive. Lactose and maltose demonstrated the lowest responses (0.350 and 0.361 μA μM^{-1} cm^{-2}). The same class distribution was observed for LOD values, which were 2.31, 2.70, and 2.72 μM for monosaccharides and 4.71 and 4.57 μM. This pattern is not an isolated slope effect; lower disaccharide response is accompanied by weaker detection reserve.

Table 1: Sugar-specific electrochemical descriptors for the NiFe nanowire calibration values.

Sugar	Class	Sensitivity (μA μM^{-1} cm^{-2})	Repeatability (%)	Reproducibility (%)	LOD (μM)	LOQ (μM)
Glucose	Mono	0.710	1.32	6.20	2.31	7.74
Fructose	Mono	0.610	5.03	7.30	2.70	8.15
Galactose	Mono	0.608	2.55	10.30	2.72	8.20
Lactose	Di	0.350	4.97	5.98	4.71	14.28
Maltose	Di	0.361	4.91	6.30	4.57	13.85

Values are taken from the first common linear range of 0.05–0.3 mM.

This table sets the numerical groundwork for the rest of the paper. It is not merely the fact that the NiFe electrode is responsive; it is the fact that the same electrode creates two families of responses on the basis of the same lower calibration boundary. This phenomenon requires a priori class-wise analysis without any consideration of food matrix.

The separation of classes has direct implications in terms of reporting. Mean sensitivity for the monosaccharides was 0.6427 μA μM^{-1} cm^{-2}, while the disaccharides had 0.3555 μA μM^{-1} cm^{-2}. The ratio between the slopes is 1.81. The calibrated concentration of a disaccharide for the same current increment is therefore 1.81 times higher than the concentration of a monosaccharide. The mean LOD values have an opposite class dependency, 2.5767 μM for monosaccharides and 4.6400 μM for disaccharides. The mean LOQ values were 8.03 and 14.065 μM, respectively. While repeatability and reproducibility were satisfactory for all five carbohydrates, precision alone did not eliminate the class dependency. Molecular response and detection reserve were the key separators.

This conclusion conforms to the chemistry of the measurement. Surface redox cycling and diffusion of the analyte to active sites are typical of alkaline nickel-based carbohydrate oxidation. Sucrose produces only a very small current response before being converted with a sensitivity of 0.034 μA μM^{-1} cm^{-2}, which is more than ten times lower compared to the average of disaccharide reducing-sugars and almost twenty times lower than the average of monosaccharides [11]. Thus,

the difference between reducing and non-reducing sugars is electrochemically detectable. Within the reducing sugars class, the lower sensitivity of disaccharides can be attributed to the combination of the factors mentioned above. Disaccharide determinations are reliable but should not be lumped into the same calibration curve as glucose, fructose, and galactose.

The numerical values for calibration parameters are transformed into the graphical depiction presented in Figure 3. Common lower 0.05-0.30 mM range is visible for all five reducing sugars, while the slopes' separation is evident both in the calibration curves and lower bound markers.

The calibration panel allows seeing the class discrimination without solely using tables of numbers. The commonly used 0.05–0.30 mM range shows that the comparison is not caused by different working ranges. The reason for discrimination lies in the slope and lower bound reserve, which results in discrimination effect affecting the concentration reports in case when all sugar classes are estimated within the same nominal calibration range.

3.2. The Reliability Index (RLC) Discriminates the Most Reliable Calibration Family

The reliability index RLC is presented in Table 2. The highest value of RLC, $\Lambda_i = 0.987$, belongs to glucose due to the combination of the highest slope and the lowest LOD together with good repeatability. There is a tight pair of fructose and galactose with RLC equal to 0.884 and 0.880 correspondingly. Lactose and maltose have the third class of RLC indices: 0.611 and 0.624. The average RLC index is 0.9168 for monosaccharides and 0.6175 for disaccharides. The obtained values show that the average of monosaccharides is justified in case of glucose, fructose, galactose containing matrices.

Table 2: Reliability-Ledger Calibration values for the five sugar entries.

Sugar	Class	D_i	Q_i	P_i	Λ_i	Calibration interpretation
Glucose	Mono	21.65	6.46	0.9624	0.987	strongest single calibrant
Fructose	Mono	18.52	6.13	0.9384	0.884	monosaccharide family
Galactose	Mono	18.38	6.10	0.9358	0.880	monosaccharide family
Lactose	Di	10.62	3.50	0.9453	0.611	disaccharide family
Maltose	Di	10.94	3.61	0.9439	0.624	disaccharide family

RLC Table reduces separate validation indicators into one decision parameter, preserving the rationale behind each class distinction. High value of glucose is due to the sum of its slope and detection reserve. Disaccharides have lower values mostly because of their response intensity and LOD location. It keeps the disaccharide measurements useful, while raising doubts about unconditioned slope transfer.

RLC is not the method discovering some novel electrochemical phenomena, but the way to express the calibration decision. Laboratory could be tempted to use glucose as the only calibrant, since it shows the highest slope and the most popular target in glucose-sensor literature. It is allowable only for glucose-specific measurements. In foods, besides glucose, fructose and galactose are common monosaccharides, while milk is lactose-rich and maltose can occur in processed and enzymatically transformed products. RLC provides the class-oriented recommendation: glucose should be used for glucose-only measurement, monosaccharide slope average should be used for measuring of reducing sugars in general, and disaccharide slope should be used for dominant lactose or maltose.

The precision-retention indicators provide interesting insight. Available diffusion data of aqueous sugar solutions confirm the assumption about the possibility of the effect of the molecule size on diffusion process, so the low response intensity of disaccharides can be explained by the response intensity and access, and not just by random instability [38]. While glucose has the highest P_i, lactose and maltose do not show lack of repeatability, their P_i is similar to P_i of monosaccharides.

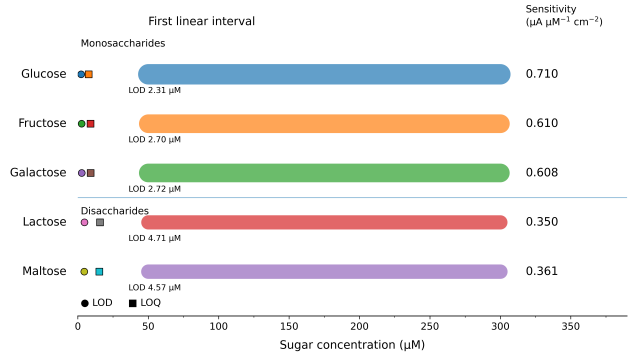

(a) Sensitivity-scaled calibration atlas.

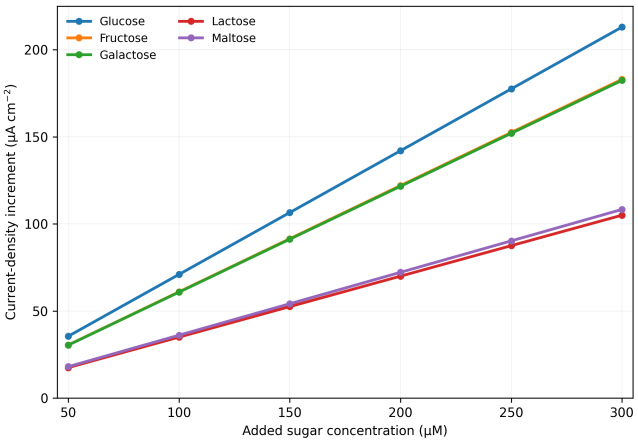

(b) Linear current-density response.

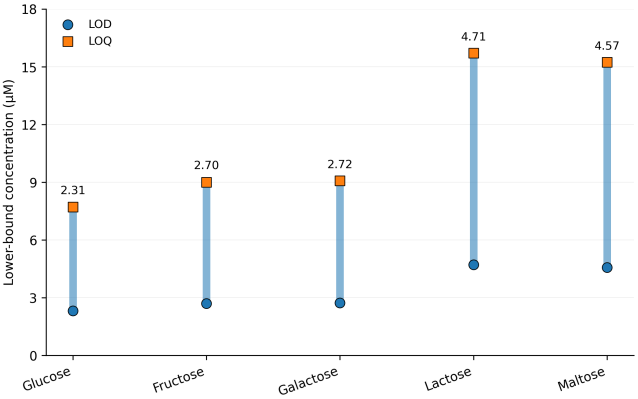

(c) LOD and LOQ profile.

Figure 3: Five-sugar calibration record.

Therefore, the low reliability of disaccharides is not the indicator of fabrication reproducibility problems. It is the problem of response and reserve. It is good for practical purposes: food analyst using the proper disaccharide calibration can have the reproducible signal. The problem is reporting, not the instable measurement.

The reliability calculation is represented in Figure 4 as analyte-specific dials, not as one ranked list. Each dial includes all three slope, detection reserve, and precision retention components in the resulting Λ_i value, providing visual evidence of high-reliability monosaccharide cluster and lower, but internally consistent disaccharide cluster.

The dial arrangement avoids making RLC too simplistic. While glucose is by far the best calibrant, fructose and galactose are sufficiently similar for them to be put into one group of monosaccharides. Lactose and maltose have formed a weaker response group without losing too much precision, and hence the low disaccharide detection performance

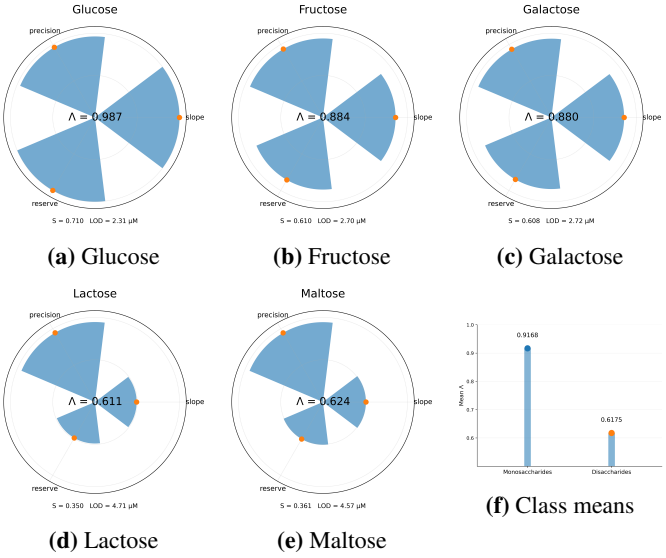

(a) Glucose **(b)** Fructose **(c)** Galactose

(d) Lactose **(e)** Maltose **(f)** Class means

Figure 4: Sugar-level RLC profiles.

is just the problem of calibration choice, not poor repeatability.

3.3. CBCE Calculates the Class-Based Concentration Penalty

The results of CBCE analysis can be found in Table 3. Multiplier of class expansion M_{CBCE} amounted to 1.808, which means that the maximum expansion equals 80.8%. Thus, a certain increment of current measured under monosaccharide calibration will be 1.808 times higher under disaccharide calibration. For any unknown food matrix, a simple concentration value cannot be used anymore; only the concentration value bounded by a certain class can serve as a valid measure. If, for instance, the same current increment corresponds to 100 μM according to the mean slope of monosaccharides, then it corresponds to approximately 181 μM according to the mean slope of disaccharides.

Table 3: Class-bound concentration envelope derived from class mean slopes.

Reporting case	Mean slope	Mean LOD	Mean LOQ	Relative concentration	Concentration expression
Known monosaccharide	0.6427	2.5767	8.030	1.000	$\Delta J/0.6427$
Known disaccharide	0.3555	4.6400	14.065	1.808	$\Delta J/0.3555$
Unknown dominant class	–	–	–	bounded interval	$[\Delta J/0.6427, \Delta J/0.3555]$

Table 3 provides what needs to be done if the product class is not known. One current increment measurement is considered a legitimate electrochemical measurement; however, its translation into the concentration becomes conditional. The bounded interval is thus a reporting tool, not a punishment to the electrode.

CBCE is particularly useful in situations with ambiguous food matrices. Fruits are usually made up of glucose and fructose; milk-based products contain mainly lactose; maltose is an essential component in cereals, brewing, and enzyme-hydrolyzed samples; and carbonated beverages may have sucrose that becomes measurable after processing. A quick screening system may not know the sugar composition unless it has some separation or enzymatic preprocessing or product information. CBCE allows an analyst to make an uncertainty statement without the need to pretend that the electrode can determine the sugar class based on a current increment measurement. This is analogous to the uncertainty-aware calibration procedure elsewhere, where the prediction should be made conditioned on the calibration conditions [32, 33].

The class-bound output also helps clarify the importance of the selectivity test. The interference experiments revealed negligible current

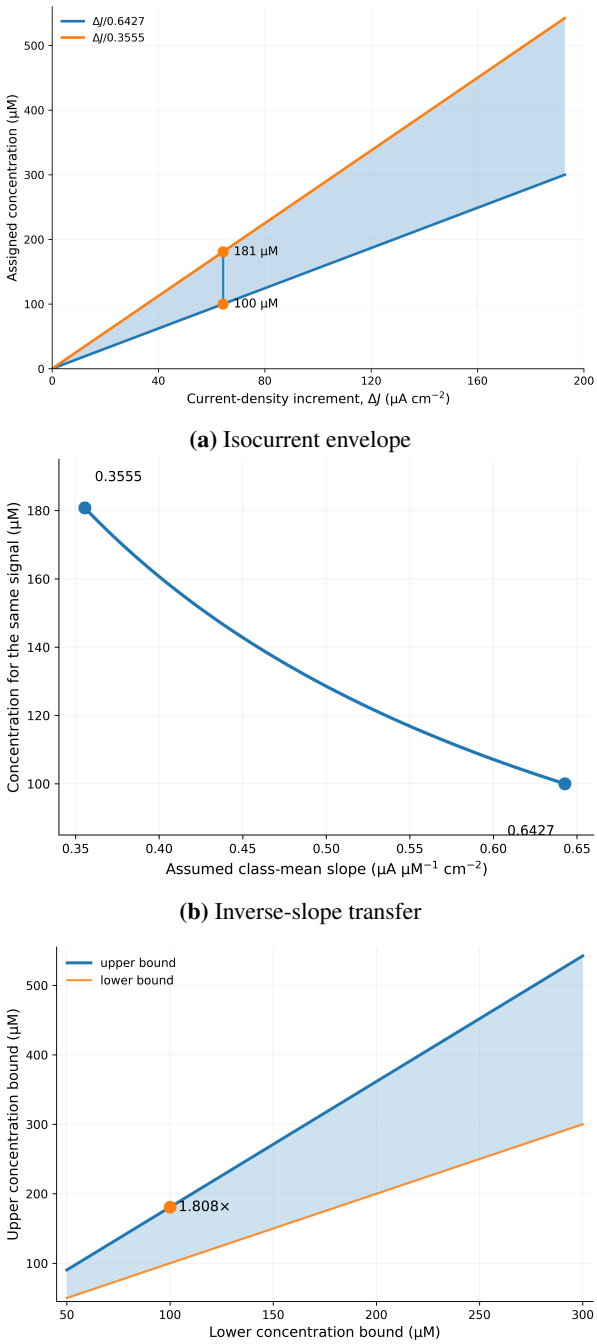

(a) Isocurrent envelope

(b) Inverse-slope transfer

(c) Bound-expansion field

Figure 5: Class-bound concentration mapping.

generation from glycerol, citric acid, Cu^{2+}, K^+, Na^+, Cl^-, Ca^{2+}, NO_3^-, Mg^{2+}, SO_4^{2-}, uric acid, ascorbic acid, gallic acid, and ethanol under the investigated conditions [11]. This selectivity result is crucial since it allows us to consider the current increment measurement as a sugar response and not as a general response to the matrix components. However, the selectivity against interference does not solve the problem of class assignment among reducing sugars. Glucose-rich and lactose-rich matrices may both lack major interference while having different concentrations. CBCE adds this class-assignment step.

The CBCE equations are plotted on the signal-concentration graph in Figure 5. The shaded area shows the bounded interval that needs to be used in case of current increment measurement when the dominating class of reducing sugars is not known.

The concentration map is the key reporting output of the unknown

class. It demonstrates that ambiguity is not some minor annotation to put into the text but shifts the upper concentration bound by 80.8%. So, an unknown food product that can exhibit ambiguous reducing-sugar dominance must receive a bounded reporting result unless its identity or composition data suggest picking one class slope.

3.4. Food-Matrix Agreement Ensures Practicality with Disciplined Reporting

The food-matrix agreement list is provided in Table 4. The direct determination of reducing sugar involved peach juice, honey, diet coke, milk, isotonic solution, and apple. The total sugar determination included peach juice, coke, diet coke, and apple. The recovery interval was from 94.10 to 105.20%. This is a very tight interval for a compact and non-enzymatic electrochemical method working on different matrices. The mean absolute residual was 3.07 percentage points. For direct reducing-sugar entries, the mean recovery was 98.05% with mean absolute residual 3.68 percentage points. For total-sugar entries, the mean recovery was 99.11% with mean absolute residual 2.14 percentage points.

Table 4: Food-matrix agreement ledger for direct reducing sugar and total sugar.

Food sample	Mode	Sensor value	Reference or label value	Recovery (%)
Peach juice	Direct RS	44.72 ± 0.40 g/L	46.88 ± 2.10 g/L	95.40
Honey	Direct RS	0.756 ± 0.030 g/g	0.790 ± 0.004 g/g	96.10
Diet coke	Direct RS	0 g/L	0 g/L	100.00
Milk	Direct RS	52.6 ± 2.3 g/L	50 g/L	105.20
Isotonic solution	Direct RS	48.8 ± 3.1 g/L	50 g/L	97.50
Apple	Direct RS	75.1 ± 0.87 mg/g	79.82 ± 15.90 mg/g	94.10
Peach juice	Total sugar	137 ± 16 g/L	140 g/L	97.85
Coke	Total sugar	123 ± 17 g/L	120 g/L	102.50
Diet coke	Total sugar	0 g/L	0 g/L	100.00
Apple	Total sugar	122 ± 0.72 mg/g	127.3 ± 29.8 mg/g	96.10

Food entries show that direct and total modes cannot be aggregated together into one category. Peach juice and apple differ in terms of readings in direct and total modes. In addition, diet cola proves that the method does not produce false sugars in a zero-sugar matrix. These samples demonstrate that food validation data is more complicated than simple glucose validation.

Food table highlights the distinction between class and mode. For example, peach juice contained 44.72 ± 0.40 g/L direct reducing sugar by the sensor and 137 ± 16 g/L total sugar after conversion. These are not competing measures of the same value. Rather, these are different questions asked of the analysis. Direct reducing sugar characterizes the fraction already measurable without conversion. On the contrary, total sugar includes substantial contribution of conversion. Apple provides the same pattern with lower gain: 75.1 ± 0.87 mg/g direct reducing sugar and 122 ± 0.72 mg/g total sugar. Therefore, the reporting of the correct measure depends on the interest of the user in reducing sugar monitoring, total sugar label equivalence, or process control.

Diet coke is a valuable negative control because it produced zero values in both modes. This sample is important because acid/heat and alkaline treatments could, in theory, produce background/matrix currents in complex beverages. The zero value indicates that the measurement procedure does not produce a false sugar signal in this matrix. As for regular coke, it appeared in total-sugar mode and gave 123 ± 17 g/L against the reference of 120 g/L with recovery of 102.50%. The result can be explained by the need to consider the non-reducing sugar conversion when sucrose or other non-reducing components are present.

The milk sample represents the class-specific calibration case because the sample was calibrated with lactose calibration since lactose is the primary reducing sugar in milk [11]. The sensor showed 52.6 ± 2.3 g/L against the reference of 50 g/L, which resulted in 105.20% recovery. If the milk had been analyzed using monosaccharide mean slope, the result would have been underestimated due to the larger mean slope translating the same current increment into a smaller concentration. Food validation results are presented in Figure 6 as agreement strips. This view preserves the integrity of each product unit and demonstrates that direct and total modes both remain close to reference or label value when appropriate reporting mode is used.

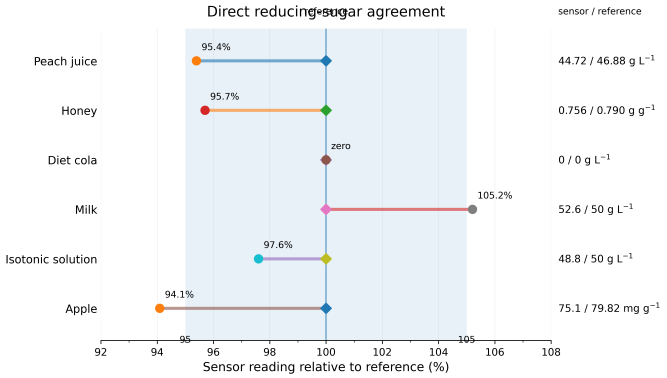

(a) Direct reducing-sugar agreement.

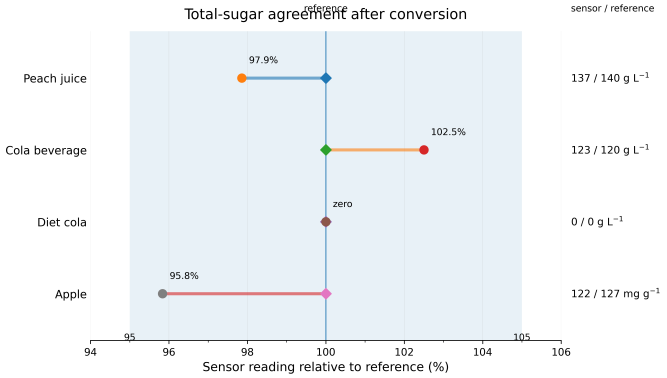

(b) Total-sugar agreement after conversion.

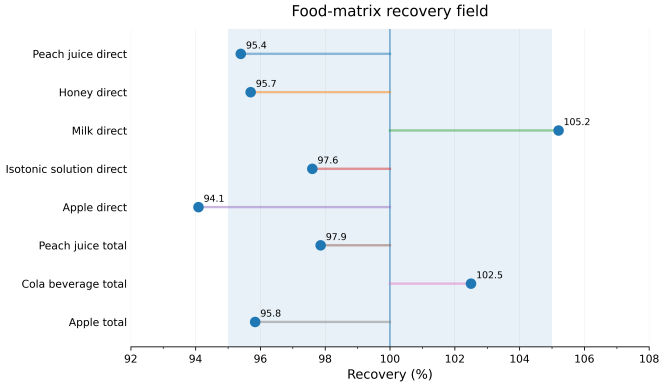

(c) Recovery concordance field.

Figure 6: Food-matrix agreement.

The agreement plots show that the reporting logic remains applicable to real foods. Recoveries close to 100% of fruit juice, honey, dairy, isotonic solution, cola, diet cola, and apple suggest that class and mode do not just improve mathematical model but retain agreement with reference or label values.

3.5. RTA Differentiates Residual Sizes with Uncertainty Considerations

The residual and recovery-tension quantities have been tabulated in Table 5. The absolute residual value of the highest magnitude was apple direct reducing sugar of -5.90%, then milk direct reducing sugar

of +5.20%, peach juice direct reducing sugar of -4.60%, and honey direct reducing sugar of -3.90%. In terms of absolute percentages, the apple and milk samples surpass the chosen interpretive band of ±5%. But when uncertainties have been considered, the two cases cannot be viewed as equal in significance. The apple direct reducing sugar had $z = -0.30$, due to its wide standard deviation of 15.90 mg/g. There was no reference standard deviation for the milk sample.

Table 5: Recovery-Tension Analysis for the food-matrix entries.

Sample	Mode	Recovery (%)	Residual ε_k (%)	T_k	z_k
Peach juice	Direct RS	95.40	-4.60	0.92	-1.01
Honey	Direct RS	96.10	-3.90	0.78	-1.12
Diet coke	Direct RS	100.00	0.00	0.00	–
Milk	Direct RS	105.20	5.20	1.04	–
Isotonic solution	Direct RS	97.50	-2.50	0.50	–
Apple	Direct RS	94.10	-5.90	1.18	-0.30
Peach juice	Total sugar	97.85	-2.15	0.43	–
Coke	Total sugar	102.50	2.50	0.50	–
Diet coke	Total sugar	100.00	0.00	0.00	–
Apple	Total sugar	96.10	-3.90	0.78	-0.18

RTA visualization converts recovery into an interpretive representation. Residual close to 5% cannot be declared unacceptable, in case if there is a considerable uncertainty in reference value; nevertheless, residual rows with no reference standard deviation call for caution. Thus, RTA provides better auditable representation of results without modifying measurement process.

The relation between percentage residuals and z_k is important for analysis. Without the context of normalized uncertainty, a reader could exaggerate the apple residual. Direct reducing sugar in apple falls outside of the chosen ±5% band, but the difference between sensor and reference is insignificant considering their combined uncertainties. On the other hand, milk has a residual above the band, but it is not accompanied by reference uncertainty to put the difference into perspective. Thus, RTA generates a more accurate interpretation: apple cannot be claimed to have poor agreement, while milk has a positive deviation and requires reference uncertainty for full understanding.

The total-sugar measurement results are especially good. The residuals for them were -2.15% for peach juice, +2.50% for coke, 0% for diet coke, and -3.90% for apple. There was no increased disagreement due to conversion. In particular, total-sugar mode generated fewer mean absolute residuals than direct reducing-sugar mode. Practically, it means that there is no extra source of disagreement in total sugar conversion, since conversion may cause errors due to hydrolysis efficiency, dilution, losses or changed matrix response. NiFe nanowires' measurements showed that acidification/heating of the sample before electrochemical measurement preserves the agreement with reference/label value in tested matrices.

RTA representation in Figure 7 splits the information about residual magnitude from its uncertainty adjustment. Direct reducing sugar in apple falls slightly outside of the nominal -5% recovery band, but the low z value proves its agreement with reference uncertainty. Entries without reference standard deviation stay on the residual shelf.

The residual fields provide additional interpretation besides recovery percentages. While the residual for apple direct reducing sugar is higher than the residual band nominal value and has a low uncertainty-normalized difference, milk provides a similar positive residual without any reference standard deviation. Both of these should be considered differently from each other and this is clear from RTA plot.

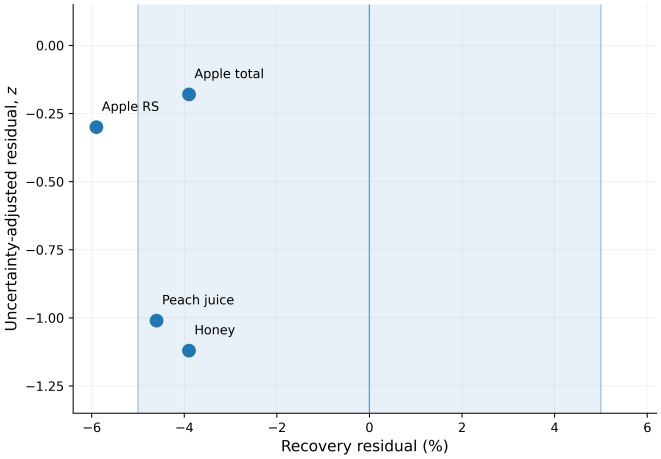

(a) Uncertainty-adjusted residuals

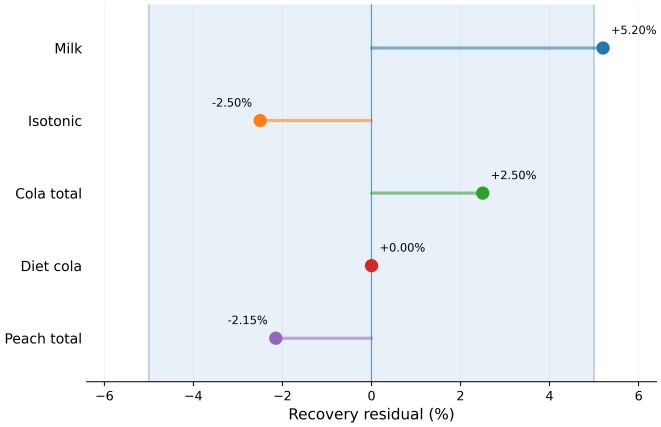

(b) Entries without reference SD

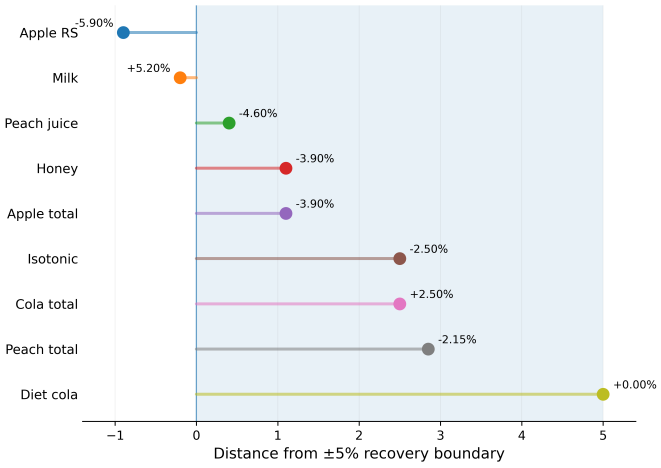

(c) Distance from the ±5% boundary

Figure 7: Recovery-tension fields.

3.6. HGP Proves that Reporting of Total Sugar is Another Chemical Mode

The HGP results for peach juice and apple are presented in Table 6. These were the two samples tested in both direct and total modes. In the case of peach juice, the sensor hydrolysis multiplier was 3.064, and the reference multiplier was 2.986. The sensor-based conversion-dependent share was 67.36% and the reference one was 66.51%. The partition difference was only 0.84 percentage points. For apple, the sensor multiplier was 1.625 and the reference multiplier was 1.595. The sensor-based conversion-dependent share was 38.44%, and the reference one was 37.30%.

Conversion is best for total sugar reporting in the HGP table because peach juice has the majority of total sugars converted, and apple juice has a smaller but still significant amount of conversion required. Consistency between sensor and reference partitions can be considered

Table 6: Hydrolysis-Gain Partitioning for matrices measured in direct and total modes.

Matrix	Sensor H_k	Reference H_k	Sensor ϕ_k	Reference ϕ_k	$\Delta\phi_k$	Interpretation
Peach juice	3.064	2.986	67.36%	66.51%	0.84 pp	conversion-dominant
Apple	1.625	1.595	38.44%	37.30%	1.14 pp	mixed direct/converted

evidence of the chemical validity of the converted values.

Conversion shifts our understanding of the total-sugar entries in the HGP table. Peach juice cannot be described as a direct reducing sugar sample with some sort of correction factor because most of its total sugar is detected after conversion only. Apple juice has fewer converting sugars but still has a sizeable amount of converted sugar fraction. Those observations further emphasize the need for food matrix and product category inclusion in the report of the portable sensor. The single concentration field will not suffice; the report needs to tell whether the reading is for direct reducing sugar or for total sugar after conversion and, in case there is an option, the hydrolysis multiplier used.

Close correspondence between sensor and reference partitions is crucial to the evaluation of conversion procedure. The conversion could provide a reasonable total sugar recovery but distort the relative relation between the fractions. In the current experiment, the sensor and reference partitions did not differ significantly in hydrolysis multipliers for the pair of matrices. That means that the conversion process is chemically consistent and does not distort the relative relation of fractions.

The direct versus conversion partition can be found in Figure 8. Peach juice has conversion-dominance, whereas apple has more direct fraction. The sensor partitions correspond well to reference partitions for both products.

This is shown by the behavior of the partition panels which demonstrates why total sugar is a unique output state: peach juice is mostly dependent on conversion-based sugar, but apple contains more direct reducing sugar. Since both the sensor and reference partitions exhibit close readings, the conversion stage is not merely a recovery improvement; it is an unveiling of a meaningful chemical fraction of total sugar pool.

3.7. Reporting Logic and Material Behaviour Reinforce Each Other

One can see that the reporting logic acquires credibility due to the correlation with the material behaviour of the electrode. Nanowire morphology enhances surface area and number of active sites, and NiFe composition facilitates redox reaction in alkaline medium. Alkaline solution in absence of sugar yielded current around 55 μA cm^{-2}, sugar additions resulted in fast increase of current, and the response time was about 6 s [11]. Diffusion effect was evident from the linear dependence of peak current density on the square root of scan rate in cyclic voltammetry. This makes class-aware calibration feasible: when transport and access are involved, differences in molecule sizes and diffusion rates should affect the slope.

The stability result adds a new dimension to deployment possibilities. Sensor sensitivity did not change during first two weeks of storage in room air, then decreased with time, and could be restored by polarizing the electrode for 45 minutes in blank solution at 0.8 V vs. SCE [11]. For the purpose of food control application, this result must be neither considered a guarantee of flawless stability nor treated as a serious drawback of the sensor. It is just a manageable restriction for deployment.

A portable food-control protocol can incorporate regular calibration or reactivation steps at certain intervals. Thus, RLC and RTA will remain traceable relative to the electrode state and its report.

The selectivity result should be considered in connection with reporting logic too. Interference results show no response to a wide range of ions and organic compounds in tested concentrations. This strengthens food-matrix claim especially for beverages and fruits-containing foods with their salt, acid and antioxidant content. However, the low response of sucrose to be converted shows that selectivity and total sugar

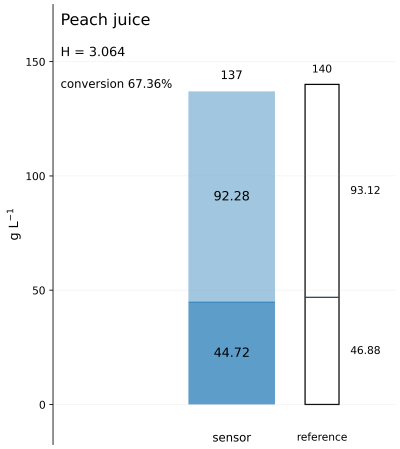

(a) Peach juice partition

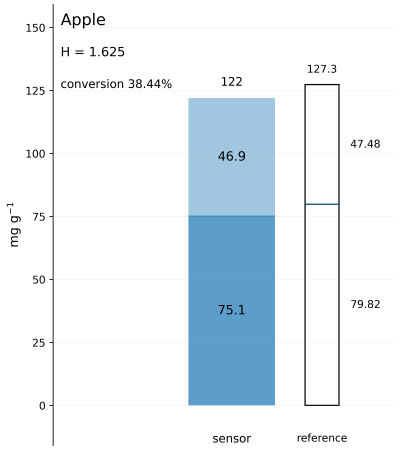

(b) Apple partition

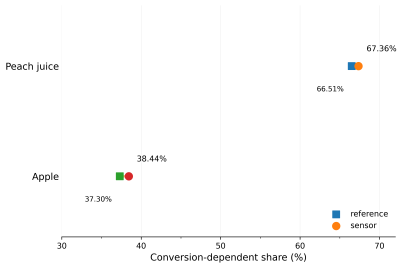

(c) Conversion-share alignment

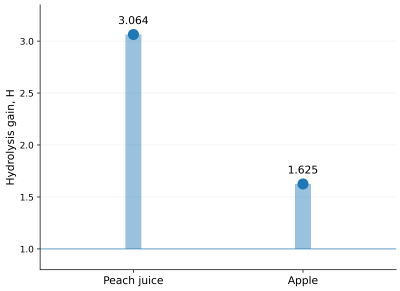

(d) Hydrolysis-gain multiplier

Figure 8: Hydrolysis-gain partitioning.

Table 7: Deployment interpretation of representative non-enzymatic sugar sensor families.

Sensor family	Main analyte coverage	Matrix orientation	Reporting implication
NiFe nanowire array	Glucose, fructose, galactose, lactose, maltose, and converted sucrose contribution	Honey, fruit, beverages, milk, isotonic solution	Broad food-screening coverage requiring class and mode labels
NiFe layered double hydroxide	Glucose	Electrochemical model solutions	Strong glucose response; narrower food-mode interpretation
NiFe-polyaniline	Glucose	Glucose-oriented validation	High glucose sensitivity; class transfer remains unresolved
NiCu or CuNi systems	Glucose and related carbohydrate targets	Biological or model matrices	Valuable bimetallic activity; total-sugar reporting depends on sample design
Nickel nanoflowers	Glucose and fructose	Juice and honey examples	Food-relevant simple-sugar capability, but less complete class coverage
NiCo nanoparticle or sulphide systems	Glucose	Biological or flexible-sensor settings	Useful for wearable or non-invasive glucose contexts; not directly equivalent to food total sugar

Table 8: Integrated reporting rule derived from RLC, CBCE, HGP, and RTA.

Analytical condition	Calculation	Reported output	Rationale
Known glucose/fructose/galactose dominance	Monosaccharide RLC slope	Class-specific reducing-sugar concentration	High class reliability and strong detection reserve
Known lactose/maltose dominance	Disaccharide RLC slope	Class-specific reducing-sugar concentration	Prevents under-reporting caused by inappropriate monosaccharide slope
Unknown dominant reducing-sugar class	CBCE interval	$\mathscr{B}(\Delta J)$	Makes class uncertainty explicit
Total sugar requested	Conversion plus HGP	Total sugar and conversion-dependent share	Separates direct reducing sugar from hydrolysis-revealed fraction
Elevated recovery residual	RTA with z_k where possible	Recovery-tension note	Distinguishes true concern from uncertainty-compatible difference

representation are not the same thing. A sensor may be selective to reducing sugars but still require hydrolysis to account for non-reducing ones. Therefore, the reporting process results in three different claims: the current is selective to the tested interferents, class-aware slopes should be used for reducing sugars, and total sugar needs conversion and HGP reporting.

3.8. Comparison with Nickel and Transition-Metal Sugar Sensors

Deployment considerations are summarized in Table 7. Some of the recent nickel or transition-metal based systems demonstrate excellent glucose sensing properties. NiFe layered double hydroxide on carbon cloth and NiFe–polyaniline facilitate further development of Fe-modified nickel sensing [27, 28]. NiCu MOF and NiCo nanoparticles expand the space of bimetallic systems [29, 30], while $CoNi_2S_4$ nanosheets and nickel nanoflowers present flexible and food-oriented configurations [31, 35]. Carbon-supported Ni/NiO composites and ordered nickel/chitosan nanowires represent further nanostructures [21, 22]. Nickel hydroxide electrodes are one more established architecture [24]. Reviews on metal, metal oxide and transition metal sensors highlight sensitivity, LOD, nanostructure and catalytic mechanism [13, 39]. Reviews on oxide/sulfide and general nanomaterial sensors focus on difficulties of transfer from controlled electrolyte to real samples of enzyme-free sensors [12, 14]. Researches on physiological condition sensing and nickel catalysts confirm the same deployment challenge [15, 17]. The NiFe nanowires are unique in that sense that they cover multiple reducing sugars, total-sugar conversion, various food matrices, interferents screening, and electrode reactivation information. The unique advantage of this system is not only a high slope; it is its capability to provide extensive food-relevant reporting.

Comparison situates the data obtained for the nanowires in context of the existing sensor literature, not falling into sensitivity-only competition. Numerous materials demonstrate excellent glucose performance, but far fewer have multiple-sugar calibration, actual food entries, conversion-calculated total sugar entries, and recovery interpretations in the same measurement set.

Comparison redefines the discussion of the sensor performance. In glucose monitoring, both the target analyte and the matrix are known in advance. In food control, the target could be an aggregate of sugars, the matrix is not constant, and the needed result is total sugar. Comparing sensors on the basis of LOD alone thus is misleading for the reader. A sensor with very low LOD in saliva/serum cannot be compared to a sensor with good total-sugar reporting in peach juice/coke. On the contrary, a sensor with slightly worse LOD can be more important if it reports reliable recovery in foods and gives a rule for conversion-dependent sugar. The NiFe nanowire measurements should thus be considered as a food-measuring record rather than as yet another glucose sensor. This is consistent with recent reviews of food-sector sensors which emphasize real-matrix validation and deployment of quality control in addition to electrolyte performance [3, 4].

Comparison also sets the analytical limits of the NiFe nanowire response. Both electrochemical arrays and multivariate analysis can discriminate sugar mixtures when measuring independent signals [25]. Multisugar biosensors and chemometric nickel complexes show an example of using additional signal structure [26, 41]. Trehalose-sensitive nickel foam and copper-nickel electrodes widen the possibilities for the analytes and matrices [37, 40]. Neutral solution transition-metal detection is an alternative approach [42]. In the current case, the NiFe nanowire signal allows reporting on the basis of sugar class: known sugar class means class slope; unresolved sugar class means CBCE interval; and total sugar with HGP information is provided for the conversion cases.

3.9. Integrated Operating Rule

Integrated operating rule in Table 8 transforms the calculation results into a worksheet or an interface of portable device. For the case of known dominant sugar class, the corresponding class slope should be used. For the unknown dominant sugar class, a concentration interval should be reported rather than single number. For the case of total sugar, conversion should be applied and the information about hydrolysis multiplier/conversion-dependent share should be given when the direct and total sugars are available. When there is recovery residual outside the selected interpretive band, it should be reported with normalized information if possible.

The reporting rule table represents the concrete implementation of the results into a laboratory report or portable-device interface: class slope if class is known, interval if class is unknown, converted value if total sugar is needed, and a note about recovery if agreement needs qualification.

The value of this reporting rule is that it corrects for three typical mistakes in reporting. The first mistake is to apply the maximum slope to all measurements. This maximizes the sensitivity but biases matrices rich in disaccharides. The second mistake is to report total sugar concentration without specifying whether conversion is applied. This misses the point that pre-treatment uncovers much of the signal, as in peach juice. The third mistake is to evaluate the recovery residuals as equal. RTA shows that the residual is always evaluated with respect to uncertainty and matrix properties. Altogether, these changes make NiFe nanowire data analysis into a concrete reporting method.

As simple as the rule is, it can be incorporated into the device without changing the electrode or using complex software. Spreadsheet computations of RLC, CBCE, HGP, and RTA can be made based on table values. The portable potentiostat might have a menu question about whether the sample is fruit-like, milk-like, unknown or total-sugar mode. Laboratory QC sheet would list the direct and total concentrations side-by-side. This is how an immediate practical application of the contribution is made. And honesty of the interpretation is preserved: the electrode gives a current response, which is interpreted as

a concentration in a class-dependent manner.
The operating rule is implemented as a compact reporting interface in Figure 9. The same current response is thus not forced into one concentration value but rather directed to a class-dependent, interval-bounded or converted total sugar concentration according to the sample data and analysis goal.

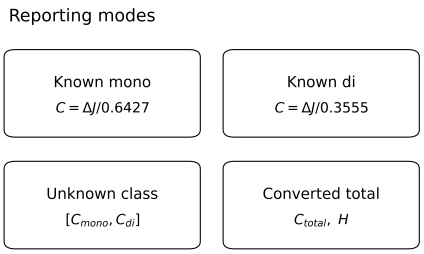

(a) Reporting console

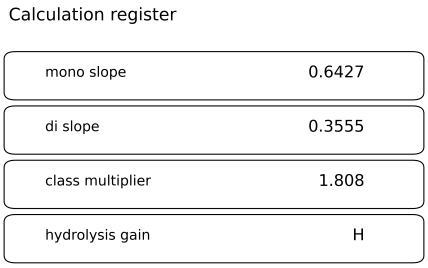

(b) Equation register

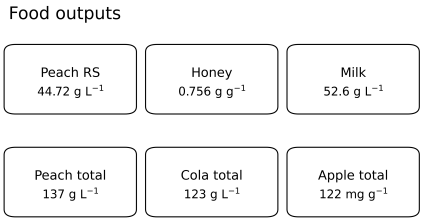

(c) Food-output cards

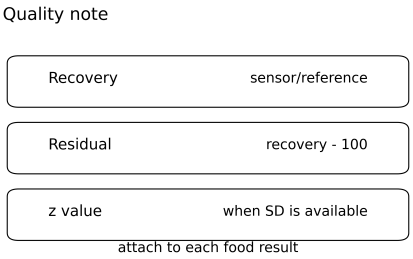

(d) Quality-note record

Figure 9: Operational reporting rule.

The reporting console reduces the paper's answer to a use rule. The same NiFe current increment may be routed to a monosaccharide concentration, a disaccharide concentration, an interval, or a total sugar value after conversion. This structure ensures that a fast response does not become disconnected from sugar class and pre-treated status.

3.10. Implications for Food-Quality Workflow

The integrated rule clarifies the method's performance in an actual food quality control workflow. One preliminary choice must be made before measuring: the analyst must determine whether the food type is of a known matrix with a known dominant reducing sugar. The milk goes directly to disaccharide calibration since lactose is the relevant reducing sugar here. Fruit and honey products may go to the monosaccharide family when the task is direct reducing-sugar screening. Beverage or fruit products where label-equivalent total sugar is desired should go through conversion first prior to the electrochemical reading. This classification is not a burden on the laboratory; it is usual product information translated into calibration logic. If the matrix category is unclear, CBCE provides a conservative reporting mode.
The second workflow implication is that dilution and calibration range should be considered as part of the reporting process. The sugar levels of real foods are high compared to the micromolar detection limits of the electrode. Food samples were diluted in 0.1 M NaOH in order to match the calibration conditions and reduce sugar levels to the analytical range [11]. For such samples, low LOD is not as important as a reliable slope, proper class assignment, and recovery in case of dilution. That is why the comparison of deployment scenarios focused on food reporting and not just submicromolar detection. Thus, a food screening readout must store the class slopes, require dilution entry, and produce a concentration with the reporting mode: direct reducing sugar, bounded reducing sugar, or total sugar after conversion.
The third implication concerns documentation. RTA makes it possible to provide a succinct quality note along with the reported result. The value with low residual and low tension can be reported without any qualifiers. The value close to the selected residual band can be reported with a short caution especially when reference uncertainty is missing. The value with a high residual but low uncertainty-adjusted difference can be described as numerically falling outside the preferred band but statistically consistent with the reference spread. This kind of reporting is consistent with method validation standards and avoids excessive confidence and unwarranted rejection of valid readings [33, 34]. In food processing plants, such notes may facilitate batch screening, incoming materials checks, and quick validation before chromatographic analysis.

3.11. Integration of the Analytical Evidence

The visual and tabular evidence make up an uninterrupted analytical argument. The materials panels describe an ordered NiFe nanowire electrode in a particular alkaline cell, whereas calibration table and atlas demonstrate that five reducing sugars have the same nominal range but do not belong to the same response family. RLC turns that differentiation into a reliability statement, and CBCE table and mapping illustrate the effect of unknown sugar class. The food ledger and agreement panels check whether the reporting logic still works in the context of actual food samples. RTA adds a note on recovery to the entries requiring careful wording, and HGP explains the chemical distinction between converted total-sugar and direct reducing-sugar values. Finally, operating table and console combine those results into a reporting rule.
The resulting integrated picture provides the answer to the research question. The NiFe nanowire electrode is rapid, sensitive, and useful in a variety of food matrices, but its most defensible output depends on whether the matrix is known to be monosaccharide-dominant, disaccharide-dominant, chemically unknown, or intentionally converted to total sugar. Thus, the evidence supports the food-quality use case where the sensor output is reported along with sugar state: known class, unknown class interval, or total sugar with conversion gain information.

4. Conclusion

The research question asked whether a NiFe nanowire chronoamperometric record could be converted into reportable food-sugar outputs that would distinguish known reducing-sugar class, unknown class, and total sugar after conversion. The answer is yes, but only when the reported concentration is linked to sugar state. The first shared calibration interval of 0.05–0.30 mM revealed a distinct class separation: glucose, fructose, and galactose had a mean sensitivity of

0.6427 μA μM^{-1} cm^{-2}, whereas lactose and maltose had a mean sensitivity of 0.3555 μA μM^{-1} cm^{-2}. This 1.81-fold slope separation implies that the same current increment cannot safely be converted to the concentration when the dominant reducing-sugar class is unknown. The RLC provided the answer for the known class: glucose was the strongest individual calibrant with $\Lambda_i = 0.987$, fructose and galactose made a high-reliability monosaccharide family with $\Lambda_i = 0.884$ and 0.880, and lactose and maltose formed a lower-response but consistent disaccharide family with $\Lambda_i = 0.611$ and 0.624. Thus, known fruit- or honey-type reducing-sugar measurements should use the monosaccharide family, while lactose- or maltose-dominant products should employ the disaccharide family. CBCE provided the answer for the unknown class: the output should be a concentration interval, not a single value, because the upper bound is 80.8% higher than the lower bound.

Food validation determined whether the reporting rule stays practical outside calibration solutions. The direct reducing-sugar determinations had 98.05% recovery, and total-sugar determinations had 99.11% recovery for matrices including peach juice, honey, diet cola, milk, isotonic solution, apple, and coke. RTA showed that the residuals close to the selected band must be interpreted using the available uncertainty. HGP answered the total-sugar aspect of the question: peach juice was a conversion-dominant sample with 67.36% of the measured total signal appearing after conversion, while apple had a lower but still notable conversion-dependent share of 38.44%. These values prove that the converted total sugar is a separate analytical state, not just a cosmetic correction to the direct reducing sugar.

The operating conclusion is thus precise: the NiFe nanowire record allows rapid food-sugar screening if the report includes one of four outputs - a monosaccharide-class concentration, a disaccharide-class concentration, a CBCE interval in case of unknown reducing-sugar class, or a converted total-sugar value with hydrolysis gain information if the pair of direct and total measurements is available. This conclusion is more definite than a simple statement of sensitivity because it prescribes the exact way in which the electrode should be used: preserve sugar class if it is known, declare class uncertainty if it is unknown, and consider hydrolysis as a separate reporting state if total sugar is desired.

Data Availability

All numerical values required to reproduce the calculations are displayed in the tables and equations.

References

[1] Scapin, T., Louie, J. C. Y., Pettigrew, S., Neal, B., Rodrigues, V. M., Fernandes, A. C., ... & da Costa Proença, R. P. (2021). The adaptation, validation, and application of a methodology for estimating the added sugar content of packaged food products when total and added sugar labels are not mandatory. Food Research International, 144, 110329.

[2] Mela, D. J., & Woolner, E. M. (2018). Perspective: total, added, or free? What kind of sugars should we be talking about?. Advances in Nutrition, 9(2), 63-69.

[3] Ghaani, M., Azimzadeh, M., Buyuktas, D., Carullo, D., & Farris, S. (2024). Electrochemical sensors in the food sector: A review. Journal of Agricultural and Food Chemistry, 72(44), 24170-24190.

[4] Shi, Z., Xia, L., & Li, G. (2023). Recent progress of electrochemical sensors in food analysis. Chemosensors, 11(9), 478.

[5] Santos, F. C. U., Paim, L. L., da Silva, J. L., & Stradiotto, N. R. (2016). Electrochemical determination of total reducing sugars from bioethanol production using glassy carbon electrode modified with graphene oxide containing copper nanoparticles. Fuel, 163, 112-121.

[6] McCormick, W., Muldoon, C., & McCrudden, D. (2021). Electrochemical flow injection analysis for the rapid determination of reducing sugars in potatoes. Food chemistry, 340, 127919.

[7] Xu, X. B., Ma, F., Yu, S. J., & Guan, Y. G. (2013). Simultaneous analysis of N^{ε}-(carboxymethyl) lysine, reducing sugars, and lysine during the dairy thermal process. Journal of dairy science, 96(9), 5487-5493.

[8] Juska, V. B., Maxwell, G. D., & O'Riordan, A. (2023). Microfabrication of a multiplexed device for controlled deposition of miniaturised copper-structures for glucose electro-oxidation in biological and chemical matrices. Biosensors and Bioelectronics: X, 13, 100315.

[9] Akyüz, E., Başkan, K. S., Tütem, E., & Apak, R. (2021). High performance liquid chromatographic method with post-column detection for quantification of reducing sugars in foods. Journal of Chromatography A, 1660, 462664.

[10] Hernández-López, A., Sanchez Felix, D. A., Zuniga Sierra, Z., Garcia Bravo, I., Dinkova, T. D., & Avila-Alejandre, A. X. (2020). Quantification of reducing sugars based on the qualitative technique of Benedict. ACS omega, 5(50), 32403-32410.

[11] Patella, B., Moukri, N., Mazzara, F., Carbone, S., Oliveri, R. L., Aiello, G., ... & Inguanta, R. (2025). Sensitive electrochemical detection of total sugars in food using NiFe alloy nanowires. Microchimica Acta, 192(12), 819.

[12] Zhu, H., Shi, F., Peng, M., Zhang, Y., Long, S., Liu, R., ... & Yang, Z. (2025). Non-enzymatic electrochemical glucose sensors based on metal oxides and sulfides: recent progress and perspectives. Chemosensors, 13(1), 19.

[13] Li, H., Xiao, N., Jiang, M., Long, J., Li, Z., & Zhu, Z. (2025). Advances of transition metal-based electrochemical non-enzymatic glucose sensors for glucose analysis: a review. Critical Reviews in Analytical Chemistry, 55(6), 1099-1135.

[14] Yu, Y., Sang, M., & Liu, Y. (2025). Recent Advances of Nanomaterials in Electrochemical Enzyme-Free Glucose Sensors. Food Bioengineering, 4(4), 511-545.

[15] Osuna, V., Aparicio Martínez, E. P., Dominguez, R. B., & Vega Rios, A. (2024). A review on the advances in nanomaterials for electrochemical non-enzymatic glucose sensors working in physiological conditions. Chemosensors, 12(8), 159.

[16] Toghill, K. E., & Compton, R. G. (2010). Electrochemical non-enzymatic glucose sensors: a perspective and an evaluation. International Journal of electrochemical science, 5(9), 1246-1301.

[17] Franceschini, F., & Taurino, I. (2022). Nickel-based catalysts for non-enzymatic electrochemical sensing of glucose: A review. Physics in Medicine, 14, 100054.

[18] Bao, F., Kemppainen, E., Dorbandt, I., Xi, F., Bors, R., Maticiuc, N., ... & Calnan, S. (2021). Host, suppressor, and promoter—the roles of Ni and Fe on oxygen evolution reaction activity and stability of NiFe alloy thin films in alkaline media. ACS Catalysis, 11(16), 10537-10552.

[19] Zhang, J., Winkler, J. R., Gray, H. B., & Hunter, B. M. (2021). Mechanism of nickel–iron water oxidation electrocatalysts. Energy & Fuels, 35(23), 19164-19169.

[20] Mousty, C., & Farhat, H. (2023). Recent advances in layered double hydroxides-based electrochemical sensors: Insight in transition metal contribution. Electroanalysis, 35(7), e202200527.

[21] Ramu, J., Ramasundaram, S., Yellappa, S., Gunamalai, L., Kamilya, T., Afzal, M., ... & Vishwanath, R. S. (2024). Carbon-supported nickel/nickel oxide nanohybrid composite as a high-performance sensor for electrochemical non-enzymatic glucose detection. New Journal of Chemistry, 48(31), 13814-13824.

[22] Gonzales, V., Rightsell, C., Betancourt, A. M., & Nash, K. L. (2024). Non-enzymatic glucose detection via ordered 2D arrays of nickel and nickel chitosan nanowires. Sensors and actuators reports, 8, 100249.

[23] Yin, J., Zhang, H., Wang, Y., Dong, Y., Hasebe, Y., & Zhang, Z. (2025). Noninvasive detection of glucose using electrodeposited NiCo nanoparticles on a silk derived carbon. Journal of Alloys and Compounds, 1014, 178716.

[24] Dulgerbaki, C. (2025). Construction of nickel hydroxide based electrode material and its performance for non-enzymatic glucose sensing applications. Journal of Inorganic and Organometallic Polymers and Materials, 35(8), 7110-7128.

[25] Fang, X., Chen, J., Jiang, C., Mei, Z., Yi, X., Gao, Y., ... & Lou, X. (2021). Design of electrochemical sensor array utilizing metal materials and applications in sugar content analysis from mixtures. International Journal of Food Properties, 24(1), 984-996.

[26] Revenga-Parra, M., Robledo, S. N., Martínez-Periñán, E., González-Quirós, M. M., Colina, A., Heras, A., ... & Lorenzo, E. (2020). Direct determination of monosaccharides in honey by coupling a sensitive new Schiff base Ni complex electrochemical sensor and chemometric tools. Sensors and Actuators B: Chemical, 312, 127848.

[27] Song, D., Wang, L., Wang, B., Yu, J., Li, Y., Qu, Y., ... & Miao, X. (2020). Three-dimensional hierarchical structure NiFe layered double hydroxides nanosheets based on carbon cloth for high performance non-enzymatic glucose detection. International Journal of Electrochemical Science, 15(3), 1949-1963.

[28] Lakhdari, D., Guittoum, A., Benbrahim, N., Belgherbi, O., Berkani, M., Vasseghian, Y., & Lakhdari, N. (2021). A novel non-enzymatic glucose sensor based on NiFe (NPs)–polyaniline hybrid materials. Food and Chemical Toxicology, 151, 112099.

[29] Pan, W., Zheng, Z., Wu, X., Gao, J., Liu, Y., Yuan, Q., & Gan, W. (2021). Facile synthesis of 2D/3D hierarchical NiCu bimetallic MOF for non-enzymatic glucose sensor. Microchemical Journal, 170, 106652.

[30] Wang, J., Liu, Y., Cheng, L., Chen, R., & Ni, H. (2020). Quasi-aligned nanorod arrays composed of Nickel–Cobalt nanoparticles anchored on TiO2/C nanofiber arrays as free standing electrode for enzymeless glucose sensors. Journal of Alloys and Compounds, 821, 153510.

[31] Dong, M., Hu, H., Ding, S., Wang, C., & Li, L. (2021). Flexible non-enzymatic glucose biosensor based on CoNi2S4 nanosheets grown on nitrogen-doped carbon foam substrate. Journal of Alloys and Compounds, 883, 160830.
[32] Allegrini, F., & Olivieri, A. C. (2014). IUPAC-consistent approach to the limit of detection in partial least-squares calibration. Analytical chemistry, 86(15), 7858-7866.
[33] Magnusson, B. (2014). The fitness for purpose of analytical methods: a laboratory guide to method validation and related topics (2014).
[34] Stafiński, M., Wieczorek, M., Janicki, P., & Kościelniak, P. (2012). Theoretical and experimental examination of recovery in the context of trueness of analytical results. Talanta, 96, 39-43.
[35] Pérez-Fernández, B., Martín-Yerga, D., & Costa-García, A. (2016). Electrodeposition of nickel nanoflowers on screen-printed electrodes and their application to non-enzymatic determination of sugars. RSC advances, 6(87), 83748-83757.
[36] Shamsipur, M., Najafi, M., & Hosseini, M. R. M. (2010). Highly improved electrooxidation of glucose at a nickel (II) oxide/multi-walled carbon nanotube modified glassy carbon electrode. Bioelectrochemistry, 77(2), 120-124.
[37] Fang, X., Mei, Z., Chen, J., Xiong, S., Ning, J., Jiang, C., ... & Hui, G. (2021). A trehalose quantitative sensor based on Ni foam material modified with graphene oxidated and non-linear analysis model. Food analytical methods, 14(9), 1977-1985.
[38] Sano, Y., & Yamamoto, S. (1993). Mutual diffusion coefficient of aqueous sugar solutions. Journal of chemical engineering of Japan, 26(6), 633-636.
[39] Naikoo, G. A., Salim, H., Hassan, I. U., Awan, T., Arshad, F., Pedram, M. Z., ... & Qurashi, A. (2021). Recent advances in non-enzymatic glucose sensors based on metal and metal oxide nanostructures for diabetes management-a review. Frontiers in Chemistry, 9, 748957.
[40] Goodnight, L., Butler, D., Xia, T., & Ebrahimi, A. (2021). Non-enzymatic detection of glucose in neutral solution using PBS-treated electrodeposited copper-nickel electrodes. Biosensors, 11(11), 409.
[41] Vargas, E., Gamella, M., Campuzano, S., De Prada, A. G. V., Ruiz, M. A., Reviejo, A. J., & Pingarrón, J. M. (2013). Development of an integrated electrochemical biosensor for sucrose and its implementation in a continuous flow system for the simultaneous monitoring of sucrose, fructose and glucose. Talanta, 105, 93-100.
[42] Zhang, J., Xie, Y., Han, W., Hui, G., Zheng, Y., Ye, Q., ... & Wu, P. (2023). Study on the non-enzymatic electrochemical glucose quantitative detection method in Na2S2O3 neutral solution environment. International Journal of Food Properties, 26(2), 3177-3186.